Hindawi
Shock and Vibration
Volume 2018, Article ID 8043410, 10 pages
https://doi.org/10.1155/2018/8043410

Research Article

Prediction of Crushing Response for Metal Hexagonal Honeycomb under Quasi-Static Loading

Xinyu Geng,[1] Yufei Liu,[1] Wei Zheng,[1] Yongbin Wang,[2] and Meng Li[1]

[1]*Qian Xuesen Laboratory of Space Technology, China Academy of Space Technology, Youyi Street No. 104, Haidian, Beijing 100094, China*
[2]*Beijing Institute of Mechanics & Electricity, China Academy of Space Technology, Youyi Street No. 104, Haidian, Beijing 100094, China*

Correspondence should be addressed to Meng Li; limeng@qxslab.cn

Received 15 June 2018; Accepted 2 August 2018; Published 13 September 2018

Academic Editor: Toshiaki Natsuki

To provide a theoretical basis for metal honeycombs used for buffering and crashworthy structures, this study investigated the out-of-plane crushing of metal hexagonal honeycombs with various cell specifications. The mathematical models of mean crushing stress and peak crushing stress for metal hexagonal honeycombs were predicted on the basis of simplified super element theory. The experimental study was carried out to check the accuracy of mathematical models and verify the effectiveness of the proposed approach. The presented theoretical models were compared with the results obtained from experiments on nine types of honeycombs under quasi-static compression loading in the out-of-plane direction. Excellent correlation has been observed between the theoretical and experimental results.

1. Introduction

With increased competition being placed on the transportation industry, an increasing number of transportation vehicle manufacturers are looking for advanced buffering structures to make their vehicles light and small. Metal honeycomb structure, a classic type of cellular structure, has long been recognized as an excellent lightweight structural material due to its properties of low density, stiffness, controllable deformation, and high-energy absorption [1–4]. One practical application for metal hexagonal honeycomb structures is energy absorbers, which are frequently adopted in the automotive industry [5–8]. This type of metal honeycomb structure has also been used as a shock absorber in the Apollo 11 landing module [3].

For a considerable understanding of the crashworthy behavior of metal honeycombs, comprehensive studies have been conducted using analytical, numerical, and experimental methods. Initially, Mc Farland [9] presented a semiempirical model to predict the crushing stress of hexagonal cell structures subjected to axial loading, which is the basic idea in the understanding of crush strength for honeycombs. Thereafter, Wierzbicki [3] predicted the axial mean crushing stress of hexagonal honeycomb structures based on super folding element theory and explained that the buckling of the cell wall was attributable to plastic flow over a toroidal surface. In a followed-up study, Wu and Jiang [10] and Liaghat and Alavinia [11] focused on theoretical studies about the wavelength of the honeycomb folding mode. Recently, a simplified approach to derive the analytical solution of the mean crushing force of multicell thin-walled structures has been developed by Chen and Wierzbicki [12]. They proposed a basic folding element consisting of four extensional triangular elements and four stationary hinge lines, which is different from previous models with trapezoidal, toroidal, conical, and cylindrical surfaces with moving hinge lines. A simplified approach was also used by Zhang et al. [13, 14], and Yin and Wen [15] to predict the mean crushing stress of different topological honeycomb structures. Moreover, with simulation techniques improved, numerical simulation has been used to investigate the crashworthiness of honeycombs [16, 17]. Yamashita and Gotoh [16] investigated the effect of cell shape and foil thickness on crush behavior by numerical simulation, impact, and quasi-static experiments.

Aktay et al. [17] proposed several different numerical simulation methods of quasi-static compression and made experimental studies on honeycomb structures. Certain researchers also focused their studies on other topological honeycombs [18–20]. Zhang et al. [21] performed design optimization for the energy absorption of bitubal hexagonal columns with honeycomb core under dynamic axial crushing. Moreover, various experimental studies on the quasi-static and dynamic crush behaviors of honeycombs under out-of-plane compressive loads have been reported [16, 22–25]. The testing results corroborated that the dynamic crushing force was generally bigger than the quasi-static one. The dynamic test results affirmed that honeycomb structures have similar characteristics under quasi-static loading. Hence, analyzing the crushing properties of metal honeycomb structures with quasi-static load is essential.

This study analytically and experimentally investigated the out-of-plane crushing of metal hexagonal honeycombs with various cell specifications. The mathematical models of mean crushing stress and peak crushing stress for metal hexagonal honeycombs were predicted. In addition, the accuracy of the models was validated by comparing with the experimental results. Therefore, the analytical solutions complied with the experimental results well.

2. Theoretical Analysis

The commercial finite element codes can simulate the entire deformation process of honeycombs with various cell specifications [26–30]. However, the theoretical expressions can give a direct prediction and can be employed when no computer is available [15]. This study focused on adhesively bonded metal hexagonal honeycombs. By taking certain assumptions, we presented a simplified analysis model to describe the collapse of hexagonal honeycombs. As adopted by most researchers in the theoretical analysis of the progressive buckling of honeycomb structures, rigid-perfectly plastic material and constant local buckling wavelength $2H$ assumptions were made in the analysis. Figure 1 exhibits that every basic element will deform at the middle point during the deformation process, which can be called "plastic hinge."

We take a single "Y" cross-sectional column model that can well predict the crush behavior to analyze the properties of hexagonal honeycombs. Single- and double-foil portions of the cell walls were also accounted. Figure 2 depicts that each "Y"-shaped cellular cell has two t thicknesses and $l/2$ length and one $2t$ thickness and $w/2$ length simple super folded element. Figure 2(a) shows the cross-section configuration of hexagonal honeycombs, and that the angle between the adjacent cells is α. Figures 2(b) and 2(c) illustrate the cross section and stereogram of "Y"-shaped cellular cells. We also assumed that, during the entire deformation process, honeycomb structures will not be broken and that the influence on honeycomb mechanical properties from adhesion is not considered.

2.1. Mean Crushing Stress. Chen and Wierzbicki adopted a simplified approach for deriving the analytical solution of the mean crushing stress of thin-walled structures. To apply the super folding element method to the thin-walled structures, they proposed a basic folding element with C length and $2H$ height. The basic folding element absorbs energy from bending and deformation. Figure 3 shows two modes of energy absorption for a simple folding element, with each basic folding element containing four extensional triangles and four static plastic hinge lines. For the bending absorption mode, four static plastic hinge lines rotate θ to absorb energy, and the deforming mode absorbs energy from the deformation of four extensional triangles.

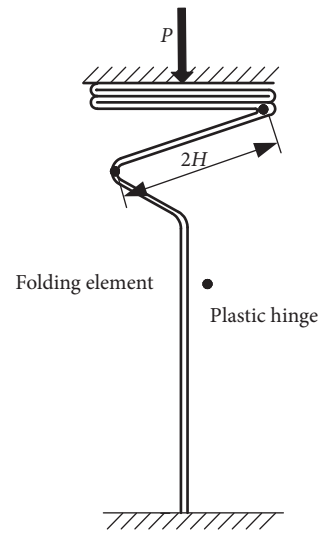

Figure 1: Plastic hinge model of metal honeycombs.

Figure 3 depicts that the energy equilibrium of one wavelength of "Y"-shaped cellular cells during the process of progressive folding can be expressed as follows:

$$F_{\mathrm{m}} \cdot 2H \cdot k = E_{\mathrm{b}} + E_{\mathrm{m}}, \tag{1}$$

where F_{m} denotes the mean force, k is the axial displacement rate, E_{b} is the bending energy, and E_{m} is the membrane energy.

The bending energy can be calculated by summing up the energy dissipation at four stationary hinge lines. Given the adhesive technology, "Y"-shaped cellular cells have one basic folding element with a thickness of $2t$ and two basic folding elements with a thickness of t; hence, the bending energy can be shown as follows:

$$E_{\mathrm{b}} = 2\sum_{i=1}^{4} M_0' \theta_i C + \sum_{i=1}^{4} M_0'' \theta_i C, \tag{2}$$

where M_0' denotes the fully plastic bending moment of the t thickness element, M_0'' is the fully plastic bending moment of the $2t$ thickness element, and θ_i is the rotation angle at each hinge line.

The fully plastic bending moment has two expressions. One is based on the Tresca yield criterion and can be shown as follows:

$$M_0 = \frac{1}{4}\sigma_0 t^2. \tag{3}$$

In a simple super folding element method, σ_0 is the flow stress with a power hardening law:

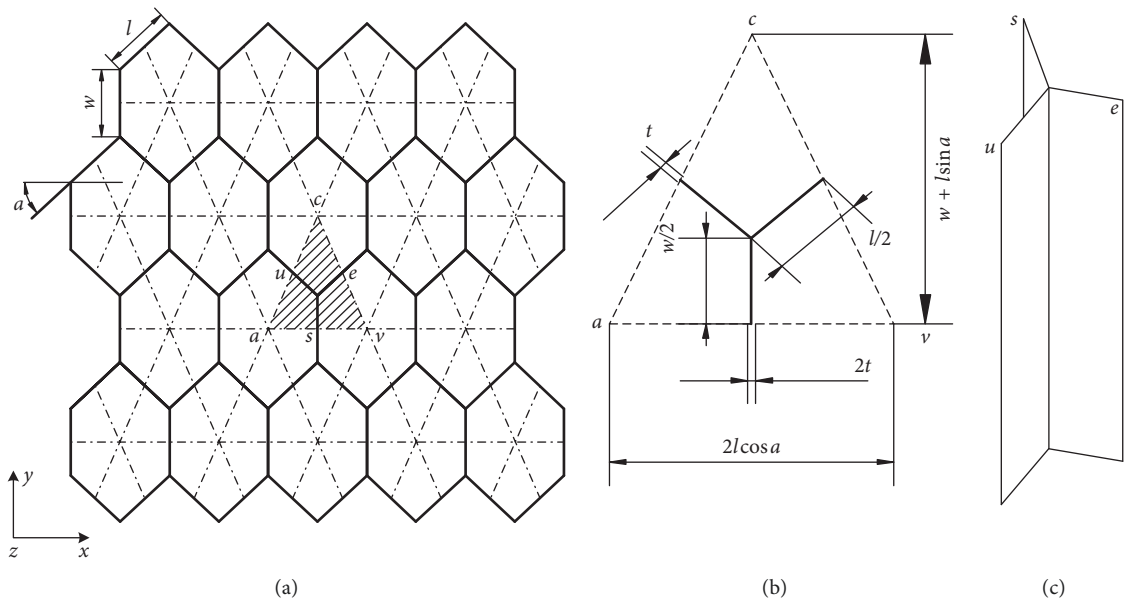

Figure 2: Analytical model of hexagonal honeycomb structures. (a) Sectional view of hexagonal honeycomb structures. (b) Sectional view of a "Y" cell model. (c) "Y" cell model map.

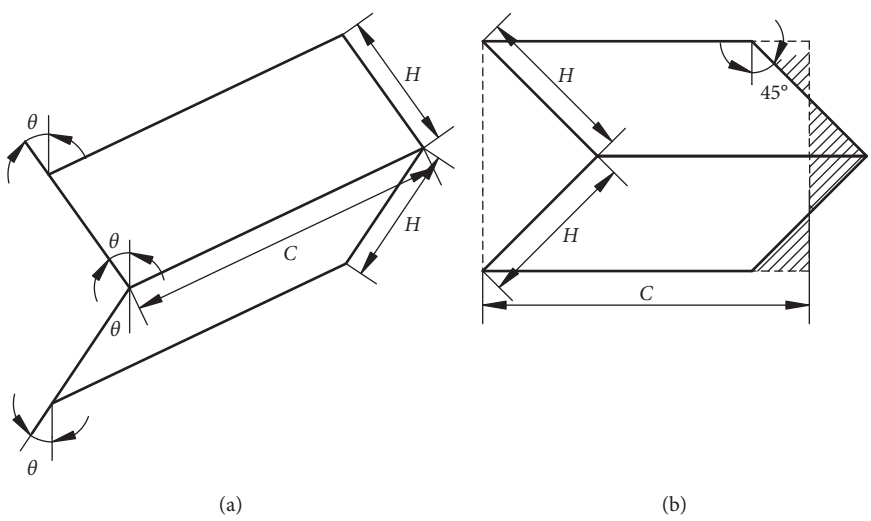

Figure 3: Simple super folding element model. (a) Bending absorption mode. (b) Deforming absorption mode.

$$\sigma_0 = \sqrt{\frac{\sigma_y \sigma_u}{1+n}}, \tag{4}$$

where σ_y and σ_u denote the yield stress and ultimate strength of the material, respectively, and n is the exponent of the power law. For the reason that the materials of the metal honeycomb have high plasticity, the metal honeycomb material can be regarded as an ideal elastic-plastic material. Therefore, the yield stress is the stress of this material when its corresponding value stops increasing after yield.

However, quasi-static crush tests corroborate that the material hardening has little influence on honeycomb mechanical properties; thus, we took the honeycomb basis material yield stress as σ_0.

In a wavelength "Y"-shaped cellular cell, the bending energy is as follows:

$$E_b = 2\sum_{i=1}^{4}\left(\frac{1}{4}\sigma_0 t^2\right)\theta_i \frac{l}{2} + \sum_{i=1}^{4}\left[\frac{1}{4}\sigma_0 (2t)^2\right]\theta_i \frac{w}{2}. \tag{5}$$

The membrane energy can be calculated by integrating the extensional and compressional areas:

$$E_m = 2\int \sigma_0 t \, ds + \int \sigma_0 (2t) \, ds. \tag{6}$$

Equations (5) and (6) affirm that the mean force F, which means the average value of resistance force in honeycomb deformation, can be obtained as follows:

$$F = \frac{\left(2\sigma_0 t H^2 + (1/2)\pi l \sigma_0 t^2 + \pi w \sigma_0 t^2\right)}{2Hk}. \tag{7}$$

Wavelength H can be determined by the stationary condition of the mean force, namely, $\partial F/\partial H = 0$, which leads to the following:

$$H = \sqrt{\frac{1}{4}\pi l t + \frac{1}{2}\pi w t}. \tag{8}$$

Substituting Equation (7) in Equation (8), the final expression of F is as follows:

$$F = \frac{\left(\pi l \sigma_0 t^2 + \pi w \sigma_0 t^2\right)}{k\sqrt{t\pi l + 2t\pi w}}. \tag{9}$$

The mean crushing stress of "Y"-shaped cellular cells undergoing axial load is as follows:

$$\sigma_{\mathrm{m}} = \frac{F}{S} = \frac{\pi\sigma_0 t^2 l + 2\pi\sigma_0 t^2 w}{k\sqrt{\pi t l + 2\pi t w}\, l \cos\alpha\,(w + l\sin\alpha)}. \tag{10}$$

For regular hexagonal honeycomb structures, $\alpha = 30^\circ$, $w = l$, and then the mean crushing stress of regular hexagonal honeycombs can be shown as follows:

$$\sigma_{\mathrm{m}} = 3.329\sigma_0\left(\frac{t}{l}\right)^{3/2}. \tag{11}$$

Another fully plastic bending moment is based on the Mises yield criterion and can be shown as follows:

$$M_0 = \frac{\sigma_0 t^2}{2\sqrt{3}}. \tag{12}$$

Substituting Equation (12) with Equation (2) and repeating the derived process, we can get the half wavelength plastic hinge based on the Mises yield criterion:

$$H = \sqrt{\frac{\sqrt{3}}{6}\pi t l + \frac{\sqrt{3}}{3}\pi t w}. \tag{13}$$

The mean force is the following:

$$F = \frac{(\sqrt{3}/3)\pi\sigma_0 t^2 l + (2\sqrt{3}/3)\pi\sigma_0 t^2 w}{k\sqrt{(\sqrt{3}/6)\pi t l + (\sqrt{3}/3)\pi t w}}. \tag{14}$$

The mean crushing stress of hexagonal honeycombs is as follows:

$$\sigma_{\mathrm{m}} = \frac{F}{S} = \frac{(\sqrt{3}/3)\pi\sigma_0 t^2 l + (2\sqrt{3}/3)\pi\sigma_0 t^2 w}{k\sqrt{(\sqrt{3}/6)\pi t l + (\sqrt{3}/3)\pi t w}\,(l\cos\alpha\,(w + l\sin\alpha))}. \tag{15}$$

The mean crushing stress of regular hexagonal honeycombs is as follows:

$$\sigma_{\mathrm{m}} = 3.097\sigma_0\left(\frac{t}{l}\right)^{3/2}. \tag{16}$$

For the purpose of convenient analysis, Wierzbicki's model was also used for comparison. The Wierzbicki's mean crushing stress of regular hexagonal honeycombs is as follows:

$$\sigma_{\mathrm{m}} = 6.6\left(\frac{t}{l}\right)^{5/3}\sigma_0. \tag{17}$$

Taking regular hexagon metal honeycombs as examples, Figure 4 gives three calculation results on the mean crushing stress of honeycombs. The mean crushing stress values calculated by Equations (11) and (16) are less than those in Wierzbicki's model. All the mean crushing stresses can apply a power exponential equation fitting to the plateau stress vs the thickness-to-length ratio curve.

2.2. Peak Crushing Stress. When loaded in the out-of-plane direction, hexagonal honeycombs have a peak crushing stress at the initial deformation process. This peak crushing stress is commonly used as the safety assessment of buffering structures. In the existing references, the calculation formula on honeycomb peak crushing stress is semiempirical and can be expressed as follows:

$$\sigma_{\mathrm{cr}} = \frac{38.2E}{\sqrt{3}\,(1-\nu^2)}\left(\frac{t}{l}\right)^3, \tag{18}$$

where E is the elastic modulus of basic materials of honeycombs and ν is the Poisson ratio of basic materials of honeycombs.

Considerable experimental studies affirm that this semiempirical formula has low accuracy, especially in the calculation of high-density honeycomb peak crushing stress. Therefore, building constitutive models on peak crushing stress of honeycombs under out-of-plane compression is necessary.

Figure 5(a) exhibits the ideal model of the hexagonal cellular structure for elastic buckling. Given the symmetry of hexagonal honeycombs, the honeycomb structure has periodic buckling with axial loads, and the length of each buckling length is plastic hinge length. Assuming a "Y"-shaped cellular cell as a slender bar, when loaded in out of plane the slender bar will deform like a parabola line shown in Figure 5(b).

With a "Y"-shaped cellular cell as a slender bar, according to the deformation shown in Figure 5(b), the peak crushing stress of hexagonal honeycombs with out-of-plane loads can be calculated by using an energy method.

The deflection curve equation of the slender bar is as follows:

$$\tau = \delta_{\mathrm{y}}\frac{x^2}{D_{\mathrm{y}}^2}, \tag{19}$$

where τ denotes the deflection of the slender bar, x is the microdeformation on axial, δ_{y} is the maximum deflection of the slender bar, and D_{y} is the length of the slender bar, $D_{\mathrm{y}} = 2H$ (mm).

The bending moment of any section of the slender bar is as follows:

$$M_D = P\cdot\tau = P\cdot\delta_{\mathrm{y}}\frac{x^2}{D_{\mathrm{y}}^2}, \tag{20}$$

where P is the axial load.

The deformation energy from bending is as follows:

$$\Delta U = \int_0^{D_{\mathrm{y}}} \frac{M_D^2}{2EI}\,dx. \tag{21}$$

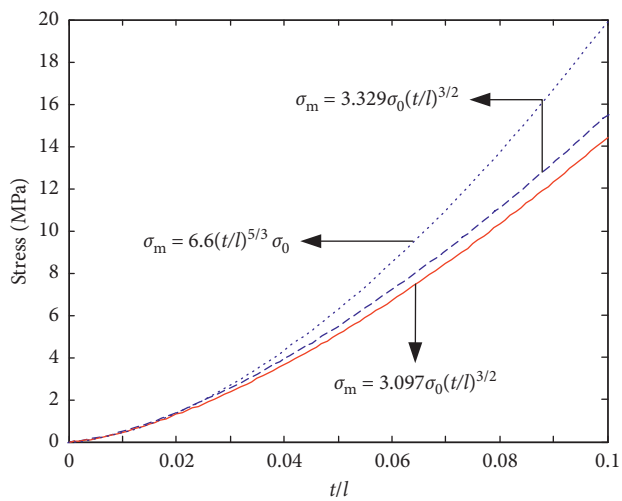

Figure 4: Three calculation models for the mean crushing stress of metal honeycombs.

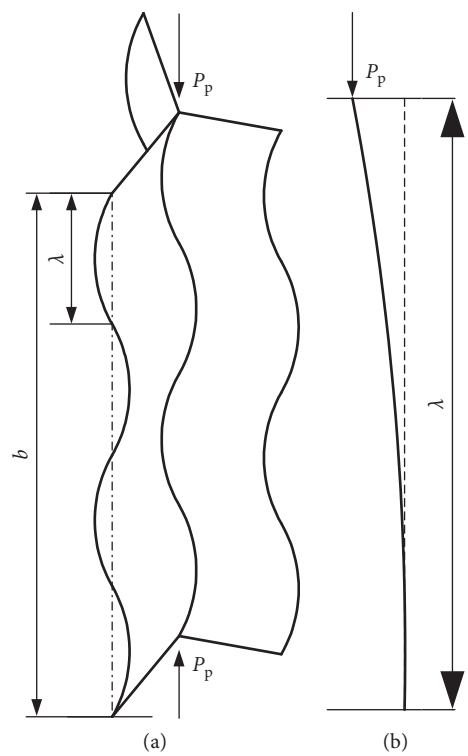

Figure 5: Elastic buckling model for the Y model of honeycombs. (a) Ideal buckling model. (b) Real elastic deformed style.

Substituting Equation (20) with Equation (21), the final expression of ΔU is as follows:

$$\Delta U = \frac{P^2 \delta_y^2 D_y}{10EI}, \tag{22}$$

where I denotes the section inertia moment of "Y"-shaped cellular cells.

Figure 2(b) affirms that the section inertia moment can be shown as follows:

$$I = \frac{1}{12} l t^3 + \frac{1}{3} w t^3. \tag{23}$$

The axial deformation of the slender bar is as follows:

$$\lambda_d = \int_0^{D_y} (ds - dx) = \int_0^{D_y} \left[\left(\sqrt{1 + \left(\frac{d\tau}{dx} \right)^2} \right) dx - dx \right], \tag{24}$$

where ds is the curvature of parabola. Equation (24) can be simplified as follows:

$$\lambda_d = \frac{2\delta_y^2}{3D_y}, \tag{25}$$

The energy from axial load during microdeformation is as follows:

$$\Delta W = P\lambda_d = \frac{2P\delta_y^2}{3D_y}. \tag{26}$$

Given that $\Delta W = \Delta U$, peak crushing load P is as follows:

$$P = \frac{20E}{3D_y^2} \left(\frac{1}{12} l t^3 + \frac{1}{3} w t^3 \right). \tag{27}$$

With the plastic hinge length model calculated by the Tresca yield criterion, the length of the slender bar is as follows:

$$D_y = 2H = \sqrt{\pi l t + 2\pi w t}. \tag{28}$$

Substituting Equation (28) with Equation (27), the final expression of peak crushing loads for honeycomb structures is as follows:

$$P = \frac{5E(lt^2 + 4wt^2)}{9(\pi l + 2\pi w)}. \tag{29}$$

Thus, the peak crushing stress of honeycombs based on the Tresca yield criterion is as follows:

$$\sigma_p = \frac{P}{S} = \frac{5E(lt^2 + 4wt^2)}{9(\pi l + 2\pi w)(l\cos\alpha(w + l\sin\alpha))}. \tag{30}$$

For regular hexagonal honeycombs, $\alpha = 30^\circ$ and $w = l$, the peak crushing stress can be shown as follows:

$$\sigma_p = \frac{100}{81\sqrt{3}\pi} E \left(\frac{t}{l} \right)^2, \tag{31}$$

The peak crushing stress for hexagonal honeycombs based on the Mises yield criterion can be shown as Equation (32) by repeating the derived process:

$$\sigma_p = \frac{P}{S} = \frac{5E(lt^2 + 4wt^2)}{2\sqrt{3}(\pi l + 2\pi w)(l\cos\alpha(w + l\sin\alpha))}. \tag{32}$$

For regular hexagonal honeycombs, the peak crushing stress is as follows:

$$\sigma_p = \frac{50}{81\pi} E \left(\frac{t}{l} \right)^2. \tag{33}$$

Taking regular hexagon metal honeycombs as examples, Figure 6 gives three calculation results on the peak crushing

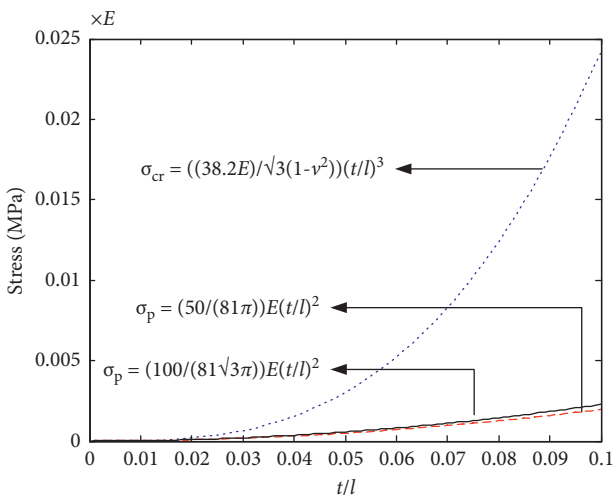

Figure 6: Three calculation models for the peak stress of metal honeycombs.

stress of honeycombs. For calculation of the peak crushing stress for classical equations, the Poisson ratio can be selected as 0.3.

3. Experimental Program and Material Properties

3.1. Experimental Program. A set of regular hexagonal honeycombs made of aluminum 3003H18 was tested to investigate the out-of-plane mechanical property of metal honeycombs. Nine types of regular hexagonal honeycombs with cell thickness of 0.04 mm, 0.05 mm, and 0.06 mm and cell lengths of 4 mm, 5 mm, and 6 mm have been used for testing. All out-of-plane crush testing was quasi-static using a 50 kN capacity Instron material testing machine with computer control and data acquisition systems. During the testing, the top platen of the machine was moved vertically downward to compress the specimens, and the loading speed was 10 mm/min. To reduce the effect of model size on results, the stress-strain curve was used to analyze instead of the load-deformation curve.

3.2. Material Properties. The material of the metal honeycomb is aluminum 3003H18, and standard tensile tests were used to establish the stress-strain curves. According to the Chinese national standard for the tensile testing of metallic materials at room temperature, tensile tests of aluminum 3003H18 foil materials with three thicknesses of 0.06 mm, 0.05 mm, and 0.04 mm were carried out. Under the condition of 20° room temperature, the tensile test is conducted in an Instron 5969 mechanical testing machine with a tensile speed of 10 mm/min. Figure 7 exhibits the test equipment and specimen.

Tensile tests were repeated four times for each thickness of aluminum foils to ensure the accuracy and reliability of the measured data. With the aluminum foil material with a thickness of 0.06 mm as an example, its quasi-static tensile mechanical test stress-strain curve is shown in Figure 8. The figure affirms that the 3003H18 material is a typical elastic-plastic material with good elasticity and plasticity. Table 1 shows the tensile test results of aluminum foils.

3.3. Experimental Investigation. Under the conditions of 20° room temperature, the test was carried out with a compression speed of 10 mm/min using an Instron 5969 type static universal mechanical testing machine for quasi-static compression. Figure 9 shows the test equipment.

The mechanical properties of the aluminum honeycomb are characterized using stress-strain curves, which can avoid being affected by the size of the specimen and obtain a unified evaluation index, to make the test result universal. Using this method, we can obtain the mean crushing stress and peak crushing stress values of nine types of honeycomb structures. Tables 2 and 3 exhibit the comparative analyses between the compression test values and the theoretical values of the nine types of honeycomb specifications.

4. Results and Discussions

For the analysis of the accuracy of the theoretical models, the deviation between the theoretical predicted values and the testing values was analyzed. Figure 10 is the deviation chart of the quasi-static mean crushing stress theoretical predicted values and tested values. With the analyzing the data in Table 2 and Figure 10, the following conclusions can be obtained:

(1) Compared with the nine tested values, the mean crushing stress theoretical predicted value of the hexagonal honeycomb structure established by the Mises yield criterion is $\sigma_m = 3.097\sigma_0 (t/l)^{3/2}$. The deviation is −3.12%~5.74%, the average deviation is 0.98%, and the standard deviation is 2.88%.

(2) The mean crushing stress theoretical predicted value of hexagonal honeycomb structure established by the Tresca yield criterion is $\sigma_m = 3.329\sigma_0 (t/l)^{3/2}$. Compared with the experimental result, the deviation is −10.83%~1.33%, the average deviation is −5.18%, and the standard deviation is −5.18%.

(3) The semiempirical model $\sigma_m = 6.6 (t/l)^{5/3}\sigma_0$ can be used to calculate the mean crushing stress given by Wierzbicki [3]. The deviation is −5.14%~8.41%, the average deviation is 3.14%, and the standard deviation is 5.07%.

The Mises yield criterion defines that, in the plastic state, the equivalent stress always equals to the flow stress, where the flow stress is characterized by the true stress rather than the nominal stress. Therefore, the mean crushing stress prediction model based on the Mises yield criterion has the highest accuracy in the three prediction models. Meanwhile, the Tresca yield criterion defines that a material will yield when maximum shear stress reaches a certain limit value. Experimental investigations corroborate that the toughness of metal materials such as aluminum, copper, and aluminum alloy complies with the Mises yield criterion well, which is the main reason that the theoretical model based on the

(a) (b)

Figure 7: Experiment for the tension test of aluminum foils. (a) Experimental instrument. (b) Experimental specimen.

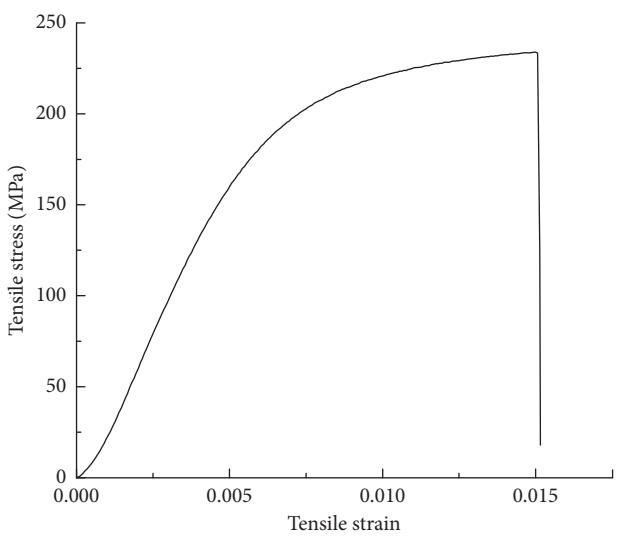

Figure 8: Stress-strain curve of aluminum foils with a thickness of 0.06 mm.

Table 1: Experimental results from tension experiments.

t (mm)	E (GPa)	σ_y (MPa)	σ_u (MPa)
0.06	38.25	140	233.8
0.05	41.73	135	268
0.04	40.39	130	219

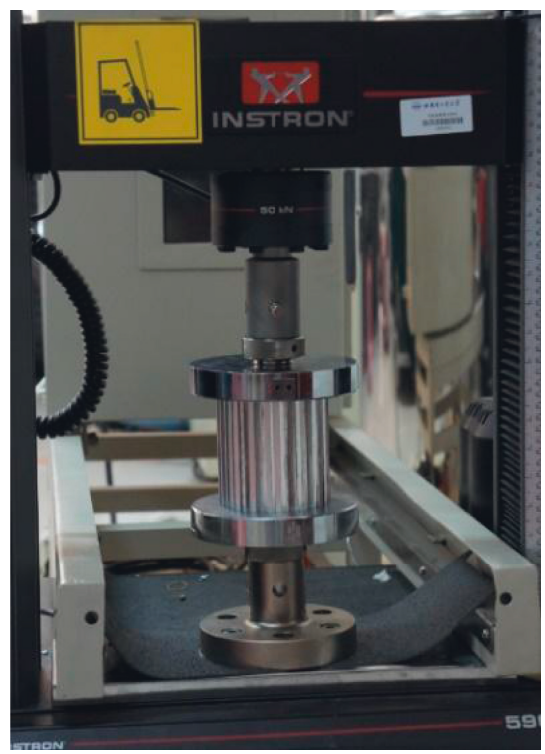

Figure 9: Quasi-static experiment instruments.

Mises yield criterion has higher calculation accuracy than that based on the Tresca yield criterion.

Figure 11 is the deviation chart of the three types of quasi-static peak crushing stress theoretical predicted values and testing values. From Figure 11 and Table 3, we can obtain the following:

(1) Compared with the nine tested values, the peak crushing stress theoretical predicted value of the

Table 2: Comparison and analysis of theoretical models for mean stress.

Number	t (mm)	l (mm)	$(\sigma_m)_t$ (MPa)	$\sigma_m = 3.097\sigma_0 (t/l)^{3/2}$ (MPa)	$\sigma_m = 3.329\sigma_0 (t/l)^{3/2}$ (MPa)	$\sigma_m = 6.6\sigma_0 (t/l)^{5/3}$ (MPa)
1	0.06	4	0.793	0.785	0.844	0.831
2	0.06	5	0.545	0.562	0.604	0.573
3	0.06	6	0.453	0.427	0.459	0.423
4	0.05	4	0.582	0.584	0.605	0.578
5	0.05	5	0.427	0.418	0.433	0.398
6	0.05	6	0.321	0.318	0.329	0.294
7	0.04	4	0.423	0.403	0.433	0.398
8	0.04	5	0.287	0.288	0.31	0.275
9	0.04	6	0.215	0.219	0.236	0.203

Table 3: Comparison of three types of theoretical models for peak stress.

Number	t (mm)	l (mm)	$(\sigma_p)_t$ (MPa)	$\sigma_p = (100/(81\sqrt{3}\pi))E(t/l)^2$ (MPa)	$\sigma_p = (50/81\pi)E(t/l)^2$ (MPa)	$\sigma_{cr} = ((38.2E)/(\sqrt{3}(1-\nu^2)))(t/l)^3$ (MPa)
1	0.06	4	1.87	1.950	1.691	3.125
2	0.06	5	1.35	1.248	1.082	1.600
3	0.06	6	0.96	0.867	0.752	0.926
4	0.05	4	1.35	1.471	1.281	1.965
5	0.05	5	0.87	0.942	0.82	1.006
6	0.05	6	0.58	0.654	0.569	0.582
7	0.04	4	0.93	0.917	0.794	0.979
8	0.04	5	0.53	0.587	0.508	0.501
9	0.04	6	0.38	0.407	0.353	0.290

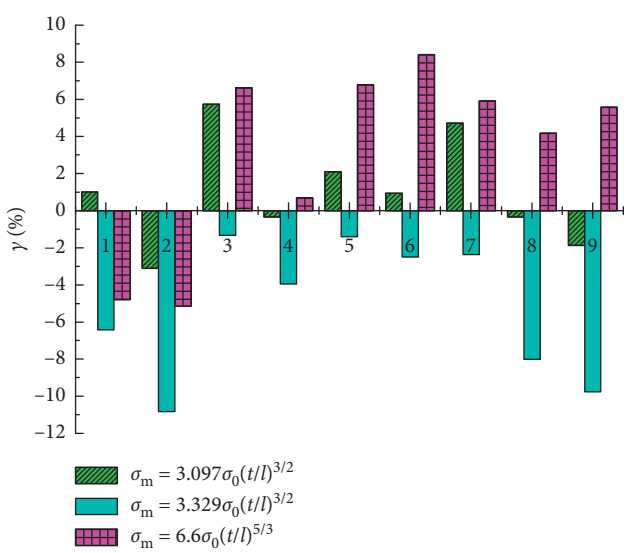

Figure 10: Histogram of the three mean crushing stress formulas with nine experimental deviations.

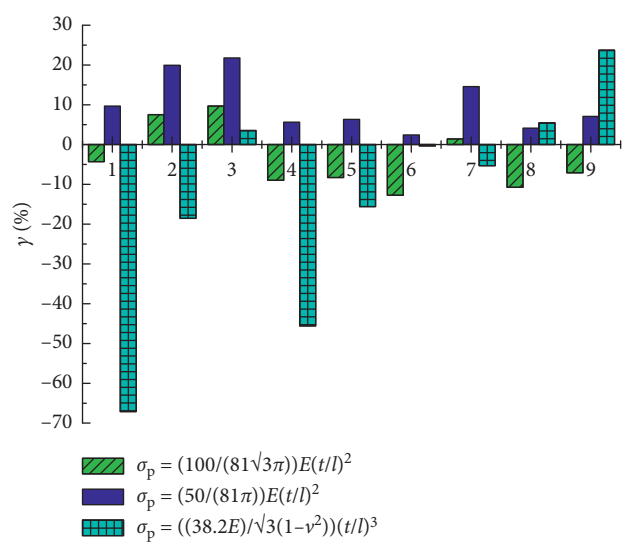

Figure 11: Histogram of the three peak stress formulas with experimental deviation.

hexagonal honeycomb structure established by the Tresca yield criterion is $\sigma_p = (100/(81\sqrt{3}\pi))E(t/l)^2$. The deviation is −12.76%~9.69%, the average deviation is −3.72%, and the standard deviation is 8.1%.

(2) The peak crushing stress theoretical predicted value of the hexagonal honeycomb structure established by the Mises yield criterion is $\sigma_p = (50/(81\pi))E(t/l)^2$. The deviation is −2.41%~21.77%, the average deviation is 10.18%, and the standard deviation is 6.99%.

(3) The peak crushing stress model of the honeycombs under the out-of-plane compression presented in the existed reference is $\sigma_{cr} = ((38.2E)/(\sqrt{3}(1-\nu^2)))((t/l))^3$. The deviation is −67.11%~23.68%, the average deviation is −13.3%, and the standard deviation is 27.85%.

The peak crushing stress prediction model based on the Tresca yield criterion has the highest accuracy in the three prediction models. The ideal buckling model for hexagonal honeycombs is shown in Figure 5(a), when honeycomb

structures' shear stress reaches the maximum value and the elastic buckling reaches the critical state. This is consistent with the yield strength definition of the Tresca yield criterion, which is why the theoretical model based on the Tresca yield criterion has higher calculation accuracy than that based on the Mises yield criterion.

5. Conclusions

In this paper, a new method to predict the mean crushing stress and peak crushing stress of metal hexagonal honeycomb structures under out-of-plane loading has been given. In addition, experimental studies for metal honeycomb structures with quasi-static loads were carried out. The analytical solutions comply with the experimental results well. Compared with the experiment results, the theoretical model of mean crushing stress based on the Mises yield criterion has a deviation ranging between −3.15% and 5.74%, the average deviation is 0.98%, and the standard deviation is 2.88%. The theoretical model of the peak crushing stress established by the Tresca yield criterion has a deviation ranging between −12.76% and 9.69%, the average deviation is −3.72%, and the standard deviation is 8.1%. These studies not only are supplements to theoretical study of metal honeycombs but also are significant in the development of different topological honeycomb structural members in the future.

Data Availability

The datasets used or analyzed during the current study are available from the corresponding author on reasonable request.

Conflicts of Interest

The authors declare that they have no conflicts of interest.

Acknowledgments

This work was supported by the National Natural Science Foundation of China (Grant nos. 51505473 and 51505028) and New Concept of Manned Lunar Landing Buffer.

References

[1] L. J. Gibson and M. F. Ashby, *Cellular Solids: Structure and Properties*, Cambridge University Press, Cambridge, UK, 1999.

[2] S.-T. Hong, J. Pan, T. Tyan, and P. Prasad, "Quasi-static crush behavior of aluminum honeycomb specimens under compression dominant combined loads," *International Journal of Plasticity*, vol. 22, no. 1, pp. 73–109, 2006.

[3] T. Wierzbicki, "Crushing analysis of metal honeycombs," *International Journal of Impact Engineering*, vol. 1, no. 2, pp. 157–174, 1983.

[4] Y. Chi, G. S. Langdon, and G. N. Nurick, "The influence of core height and face plate thickness on the response of honeycomb sandwich panels subjected to blast loading," *Materials and Design*, vol. 31, no. 4, pp. 1887–1899, 2010.

[5] C.-Z. Tsai, E. Wu, and B.-H. Luo, "Forward and inverse analysis for impact on sandwich panels," *AIAA Journal*, vol. 36, no. 11, pp. 2130–2136, 1998.

[6] A. Eskandarian, D. Marzougui, and N. E. Bedewi, "Impact finite-element analysis of slip-base sign support mechanism," *Journal of Transportation Engineering*, vol. 126, no. 2, pp. 143–153, 2000.

[7] S. Yang, C. Qi, D. Wang, R. Gao, H. Hu, and J. Shu, "A comparative study of ballistic resistance of sandwich panels with aluminum foam and auxetic honeycomb cores," *Advances in Mechanical Engineering*, vol. 5, article 589216, 2013.

[8] W. Zhang, W. Hou, P. Hu, and Z. Ma, "The nonlinear compressive response and deformation of an auxetic cellular structure under in-plane loading," *Advances in Mechanical Engineering*, vol. 7, no. 1, article 214681, 2015.

[9] R. Mc Farland, "Hexagonal cell structures under post-buckling axial load," *AIAA Journal*, vol. 1, no. 6, pp. 1380–1385, 1963.

[10] E. Wu and W.-S. Jiang, "Axial crush of metallic honeycombs," *International Journal of Impact Engineering*, vol. 19, no. 5-6, pp. 439–456, 1997.

[11] G. H. Liaghat and A. Alavinia, "A comment on the axial crush of metallic honeycombs by Wu and Jiang," *International Journal of Impact Engineering*, vol. 28, no. 10, pp. 1143–1146, 2003.

[12] W. Chen and T. Wierzbicki, "Relative merits of single-cell, multi-cell and foam-filled thin-walled structures in energy absorption," *Thin-Walled Structures*, vol. 39, no. 4, pp. 287–306, 2001.

[13] X. Zhang and H. Zhang, "Numerical and theoretical studies on energy absorption of three-panel angle elements," *International Journal of Impact Engineering*, vol. 46, pp. 23–40, 2012.

[14] X. Zhang, G. Cheng, and H. Zhang, "Theoretical prediction and numerical simulation of multi-cell square thin-walled structures," *Thin-Walled Structures*, vol. 44, no. 11, pp. 1185–1191, 2006.

[15] H. Yin and G. Wen, "Theoretical prediction and numerical simulation of honeycomb structures with various cell specifications under axial loading," *International Journal of Mechanics and Materials in Design*, vol. 7, no. 4, pp. 253–263, 2011.

[16] M. Yamashita and M. Gotoh, "Impact behavior of honeycomb structures with various cell specifications—numerical simulation and experiment," *International Journal of Impact Engineering*, vol. 32, no. 1–4, pp. 618–630, 2005.

[17] L. Aktay, A. F. Johnson, and B.-H. Kröplin, "Numerical modelling of honeycomb core crush behaviour," *Engineering Fracture Mechanics*, vol. 75, no. 9, pp. 2616–2630, 2008.

[18] H. Yin, Y. Xiao, G. Wen, Q. Qing, and X. Wu, "Crushing analysis and multi-objective optimization design for bionic thin-walled structure," *Materials and Design*, vol. 87, pp. 825–834, 2015.

[19] H. Yin, Y. Xiao, G. Wen, Q. Qing, and Y. Deng, "Multi-objective optimization for foam-filled multi-cell thin-walled structures under lateral impact," *Thin-Walled Structures*, vol. 94, pp. 1–12, 2015.

[20] Z. Zhang, S. Liu, and Z. Tang, "Crashworthiness investigation of kagome honeycomb sandwich cylindrical column under axial crushing loads," *Thin-Walled Structures*, vol. 48, no. 1, pp. 9–18, 2010.

[21] Y. Zhang, G. Sun, G. Li, Z. Luo, and Q. Li, "Optimization of foam-filled bitubal structures for crashworthiness criteria," *Materials and Design*, vol. 38, pp. 99–109, 2012.

[22] M. Z. Mahmoudabadi and M. Sadighi, "A theoretical and experimental study on metal hexagonal honeycomb crushing under quasi-static and low velocity impact loading," *Materials Science and Engineering: A*, vol. 528, no. 15, pp. 4958–4966, 2011.

[23] W. Goldsmith and J. L. Sackman, "An experimental study of energy absorption in impact on sandwich plates," *International Journal of Impact Engineering*, vol. 12, no. 2, pp. 241–262, 1992.

[24] R. Liu, C. Luo, Z. Deng, and C. Wang, "Experimental and numerical studies on aluminum honeycomb with various cell specifications under impact loading," in *Proceedings of the ASME 2008 International Mechanical Engineering Congress and Exposition*, October-November 2008.

[25] M. Z. Mahmoudabadi and M. Sadighi, "A study on the static and dynamic loading of the foam filled metal hexagonal honeycomb–theoretical and experimental," *Materials Science and Engineering: A*, vol. 530, pp. 333–343, 2011.

[26] S. Hou, Q. Li, S. Long, X. Yang, and W. Li, "Design optimization of regular hexagonal thin-walled columns with crashworthiness criteria," *Finite Elements in Analysis and Design*, vol. 43, no. 6, pp. 555–565, 2007.

[27] S. Hou, Q. Li, S. Long, X. Yang, and W. Li, "Multiobjective optimization of multi-cell sections for the crashworthiness design," *International Journal of Impact Engineering*, vol. 35, no. 11, pp. 1355–1367, 2008.

[28] H. Kurtaran, A. Eskandarian, D. Marzougui, and N. E. Bedewi, "Crashworthiness design optimization using successive response surface approximations," *Computational Mechanics*, vol. 29, no. 4-5, pp. 409–421, 2002.

[29] M. Li, R. Q. Liu, H. W. Guo, and Z. Q. Deng, "A study on out-of-plane compressive properties of metal honeycombs by numerical simulation," *Advanced Materials Research*, vol. 217-218, pp. 723–727, 2011.

[30] C. Qi, S. Yang, and R. Gao, "Numerical simulation of force enhancement by cellular material under blast load," *Advances in Mechanical Engineering*, vol. 5, article 328651, 2013.